J Solid State Electrochem (2011) 15:1149–1157
DOI 10.1007/s10008-010-1179-5

ORIGINAL PAPER

Platinum–polytyramine composite material with improved performances for methanol oxidation

Tanța Spătaru · Maria Marcu · Loredana Preda · Petre Osiceanu · Jose Maria Calderon Moreno · Nicolae Spătaru

Received: 2 June 2010 / Revised: 24 July 2010 / Accepted: 17 August 2010 / Published online: 1 September 2010

Abstract Polytyramine (PTy) is shown to be a possible alternative to other conducting polymers as a support material for fuel cell electrocatalysts such as platinum. In this work, a Pt–PTy composite was prepared via potentiodynamic deposition of polytyramine on graphite substrate, followed by the electrochemical deposition of Pt nanoparticles. The material obtained by this straightforward method exhibited, for platinum loadings as low as ca. 0.12 $mg\,cm^{-2}$, a specific electrochemically active surface area of the electrocatalyst of ca. 54 $m^2\,g^{-1}$, together with a good electrocatalytic activity for methanol oxidation in acidic media, thus ensuring better efficiency of Pt utilization. The system Pt–PTy appears to be worthy of development for methanol fuel cell applications also because the results suggested that, when deposited as small particles in a PTy matrix, platinum is less sensitive to fouling during CH_3OH oxidation.

Keywords Polytyramine · Platinum deposition · Methanol oxidation · Composite material

Introduction

It is generally accepted that extensive application of fuel cells requires electrode materials based on dispersed electrocatalytic noble metals (mainly platinum or Pt-based alloys) on a conductive, stable, high surface area substrate. One of the most widely employed supports for fuel cells is carbon black, but it was observed that this material can undergo irreversible oxidation at non-negligible rates which results in a decrease of both the electrical conductivity and the mechanical integrity of the electrode structure [1, 2]. These processes can be a problem even at the anode in direct methanol fuel cells (DMFC), particularly during fuel starvation and resulting polarity reversal [3]. This is why the use of less vulnerable to oxidation carbonaceous supports, including carbon nanotubes [4–8], carbon nanofibers [9], nonporous conductive diamond films [10–12], and conductive diamond powder [13, 14], has also been under intensive investigation.

Besides the stability of the electrode structure, another problem of major interest in current research on high-efficiency methanol fuel cells is how to minimize the loadings of noble metals while maintaining high electrocatalytic activity. An attractive way to attack both problems is to deposit such metals as small particles in a conductive polymer matrix, which allows obtaining high surface area composite materials with high catalytic activity and improved stability during methanol oxidation [15–19]. In this respect, conductive polymers of various types and pretreatments have been studied, and promising results were reported for composites based on polyaniline [20–25], polypyrrole [26–28], poly(o-phenylendiamine) [29], poly (N-acetylaniline) [30], and on copolymers of different structures [31–36].

It was found that the polymerization of monomers that contain aromatic groups directly linked to oxygen occurs more readily, resulting in polymer coatings with higher electrochemical and mechanical stability [37, 38]. Among these monomers, tyramine (Ty) (4-(2-aminoethyl)phenol) has attracted much interest mainly because its free amine group allows to purposefully modify the polymer structure

T. Spătaru · M. Marcu · L. Preda · P. Osiceanu · J. M. C. Moreno · N. Spătaru (✉)
Institute of Physical Chemistry "Ilie Murgulescu",
202 Spl. Independenței,
060021 Bucharest, Romania
e-mail: nspataru@chimfiz.icf.ro

by covalent attachment of several types of molecules and biomolecules [39]. Furthermore, it is relatively easy to deposit polytyramine (PTy) layers by electrochemical methods on various substrates, and the use for sensor applications of modified electrodes thus obtained is well substantiated [40–43].

Attempts have been also made to use PTy as a matrix for the immobilization of metal particles [44], and we have recently reported interesting electrocatalytic features of a Pt–PTy composite [45, 46]. Based upon these results, this work was aimed at evaluating the potential applications of this composite as electrode material for methanol oxidation, with an eye to possible fuel cell applications.

Experimental

The polymer matrix was electrochemically deposited on graphite (G) substrate according to a method described in the literature [44]. Prior to the deposition, the electrodes (surface area, 0.12 cm^2) were polished with alumina suspension, first with 1.0 μm for ~2 min, 0.1 μm for ~5 min, and 0.05 μm for ~5 min, followed by thorough washing with bidistilled water. The potential of the electrodes was then cycled within the range of −0.40 to 1.25 V vs. Ag/AgCl, at a scan rate of 50 $mV s^{-1}$, in a 0.1 M $HClO_4$ and 15 mM Ty (Aldrich) solution. After 30 deposition cycles, the electrodes were removed from the tyramine solution and rinsed with bidistilled water.

The PTy-modified electrodes were immersed for 10 min in a 46 mM H_2PtCl_6 solution, thoroughly washed with bidistilled water and then platinum deposition was carried out. For the reduction of the adsorbed Pt(IV), a constant potential of −0.1 V was applied to the electrode in a 0.1 M $HClO_4$ solution, and the cathodic current was recorded in order to calculate the corresponding deposition electric charge.

In some experiments electrodes obtained by the deposition of a certain amount of Pt on bare graphite substrates were also used for comparison. In those cases, the deposition was performed at the same potential (−0.1 V) from a 0.1 M $HClO_4$+2.4 mM H_2PtCl_6. For a reliable estimation of the platinum loading, prior to Pt deposition, chronoamperometric curves were recorded under the same experimental conditions in the background electrolyte both for PTy-modified and bare graphite substrates. The deposition charge was then calculated as the difference between the cathodic charge in the presence of Pt(IV) salt and that recorded in its absence. The platinum loading was controlled by adjusting the deposition time and, before further experiments, both types of electrodes (Pt/PTy/G and Pt/G) were kept for 30 min in a fresh 0.1 M $HClO_4$ solution, in order to remove remaining traces of Pt salt.

The electrochemical behavior of the composite obtained by the deposition of platinum on the PTy-modified graphite substrates was investigated by cyclic voltammetry (scan rate, 50 $mV s^{-1}$) in a 0.5 M H_2SO_4 deaerated solution, both in the absence and in the presence of CH_3OH. The oxidation of the methanol was also studied by electrochemical impedance spectroscopy (EIS), at three values of the applied potential (0.5, 0.6, and 0.7 V), within the frequency range of 10 kHz to 3 mHz and with an amplitude of the alternating signal of 10 mV. Chronoamperometric experiments were also performed at a constant potential of 0.6 V (polarization time, 60 min) in a 0.5 M H_2SO_4+3.7 M CH_3OH solution.

All the electrochemical experiments were carried out by means of a PAR 273A potentiostat in a conventional three-electrode glass cell at room temperature under deaerated conditions (high-purity nitrogen purge). A platinum gauze and a Ag/AgCl electrode (in saturated KCl solution) were used as the counter and reference electrodes, respectively. For the EIS measurements, a PAR-FRD 100 response detector was used, together with a ZSimpWin 3.21 software, and morphological observations were made after PTy and Pt deposition by scanning electron microscopy (SEM).

Surface analysis performed by X-ray photoelectron spectroscopy (XPS) was carried out on VG ESCA3 equipment, with a base pressure in the analysis chamber of 10^{-9} Torr. The X-ray source was nonmonochromatized AlK_α radiation (1,486.6 eV) with the overall energy resolution estimated at 1.2 eV by the FWHM of the Au $4f_{7/2}$ line. In order to take into account the charging effect on the measured binding energies (BEs) the spectra were calibrated using the C 1 s line (BE=285.0 eV) of the adsorbed hydrocarbon on the sample surface.

Results and discussion

Previous studies concerning the possibility of using polytyramine as a substrate for metal electrocatalysts have shown that cyclic voltammetry represents a simple method that enables better control of the polymerization process, in terms of film thickness and morphology of the PTy matrix [44]. It was also reported that, in acidic media, 20–40 deposition cycles (at a scan rate of 50 $mV s^{-1}$, within the potential range −0.40–1.25 V vs. Ag/AgCl) allow the deposition of polytyramine films with high active area and reasonably good resistivity, while further PTy deposition results in an increase of the ohmic drop without improving the active surface area of the modified electrodes [45].

For the present investigation, graphite electrodes modified by 30 PTy deposition cycles were used as support for platinum electrochemical deposition (see the "Experimental" section).

It should be noted that for efficient use of the electrocatalyst, it is advantageous to deposit it electrochemically, thereby ensuring that all the particles are in direct contact with the substrate. This is particularly important for high area supports, in which it is possible for the platinum to be deposited, yet not be in electrical contact [47]. For a value of the deposition potential of −0.1 V, the hydrogen evolution is negligible [46] and a current efficiency close to 100% is expected for the reduction of the Pt(IV) species. This is why the platinum loading of the Pt–PTy composite can be reliably calculated from the corresponding value of the deposition charge.

In order to assess the electrochemical behavior of platinum on the surface of the PTy-modified graphite, the electrodes were transferred into 0.5 M H_2SO_4 deaerated solution, and cyclic voltammograms were recorded within the −0.35–1.20 V potential range, at a scan rate of 50 mV s^{-1}, until a stable response was obtained (approximately ten cycles). Figure 1 illustrates the voltammetric behavior recorded after stabilization for PTy-coated graphite electrodes modified by the deposition of 0.12 mgcm^{-2} Pt (deposition charge, 242 mCcm^{-2}). For comparison, the inset in Fig. 1 shows a typical voltammetric response obtained under the same experimental conditions with a Pt/G electrode (Pt loading, 0.13 mgcm^{-2}). It was observed that, at the Pt/PTy/G electrodes, the shape of the voltammetric response is typical for the behavior of platinum in acidic media, although the cathodic peaks corresponding to hydrogen adsorption were somewhat drawn out, possibly due to the ohmic resistance of the polymer matrix. Nevertheless, it appears that the electrochemically active surface of the platinum deposit can be estimated from the charge associated with hydrogen adsorption, corrected for

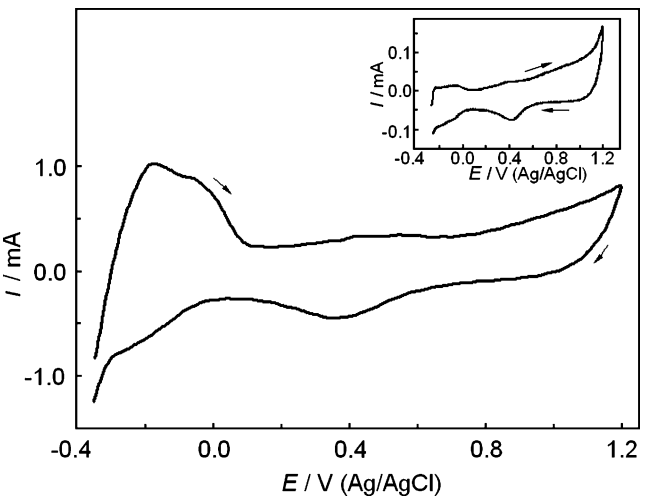

Fig. 1 Cyclic voltammogram recorded in 0.5 M H_2SO_4 deaerated solution for Pt/PTy/G electrodes. Scan rate, 50 mVs^{-1}; platinum loading, 0.12 mgcm^{-2}; geometric area, 0.12 cm^2. *Inset*: voltammetric response recorded under the same experimental conditions at a Pt/G electrode (Pt loading, 0.13 mgcm^{-2})

that for the double layer. It is worthy to note that this was not possible when using a thicker PTy matrix (40 deposition cycles), in which case for Pt loadings lower than ca. 0.25 mgcm^{-2}, hydrogen adsorption was barely distinguishable from the cathodic background [46].

For Pt/PTy/G electrodes with an average platinum loading of 0.13 mgcm^{-2}, charge integration within the 0.0 to −0.3 V potential range resulted in an average value of 14.85 mCcm^{-2}. By assuming a value of 0.21 mCcm^{-2} for a smooth platinum surface [48, 49], this charge yielded a specific surface area of ca. 54 m^2g^{-1} for Pt deposited on the PTy-covered graphite substrate. This value compares well with those reported for Pt–TiO_2 composites [50, 51], PtRu–WO_3 nanocomposite electrodes fabricated by sputtering [52], and high surface PtRu electrocatalysts, commercially available or obtained by various chemical reduction methods [53]. Conversely, as the cyclic voltammogram from the inset in Fig. 1 indicates, the specific surface area estimated by the same method for platinum electrodeposition on bare graphite was found to be much lower (ca. 4.5 m^2g^{-1} for an average loading of 0.15 mgcm^{-2}).

Figure 2 shows typical SEM images obtained for Pt/G (Fig. 2a) and Pt/PTy/G (Fig. 2b) electrodes after the stabilization of the voltammetric response. For comparison, micrographs of the two substrates, obtained at the same magnification in the absence of the Pt deposit, are also shown in the insets. It appears that on the PTy-modified graphite the electrocatalyst is well distributed on the electrode surface and the Pt particles are rather uniform in size (ranging from ca. 20 to ca. 100 nm), although clusters formation and deposition into the PTy pores are also evidenced. It was also found that, unlike the case of the Pt/PTy/G electrodes, on the bare graphite substrate the Pt particles were less uniformly distributed, and this is why micrographs like that from Fig. 2a were not used for any quantitative estimation. Nevertheless, even compared on a qualitative basis, SEM results put into evidence for the Pt/G electrodes a bigger size of the electrocatalyst particles. These features, together with the rather high roughness of the polymer coating, account for the higher specific surface area of the Pt–PTy composite. It is worthy to note that, although the above Pt/G electrodes are very far from real DMFC anodes, their use as reference material could help to understand, at least in part, the influence of the PTy intermediary layer on the electrochemical behavior of the platinum deposit.

XPS was employed in order to analyze the element surface composition and their chemical states on the surface of the electrocatalysts. Figure 3 shows the narrow-scan spectra in the Pt 4f region both for Pt/G and Pt/PTy/G electrodes. It was observed that, for the platinum nanoparticles electrochemically deposited on the bare graphite substrate, the Pt 4f spectrum could be deconvoluted into

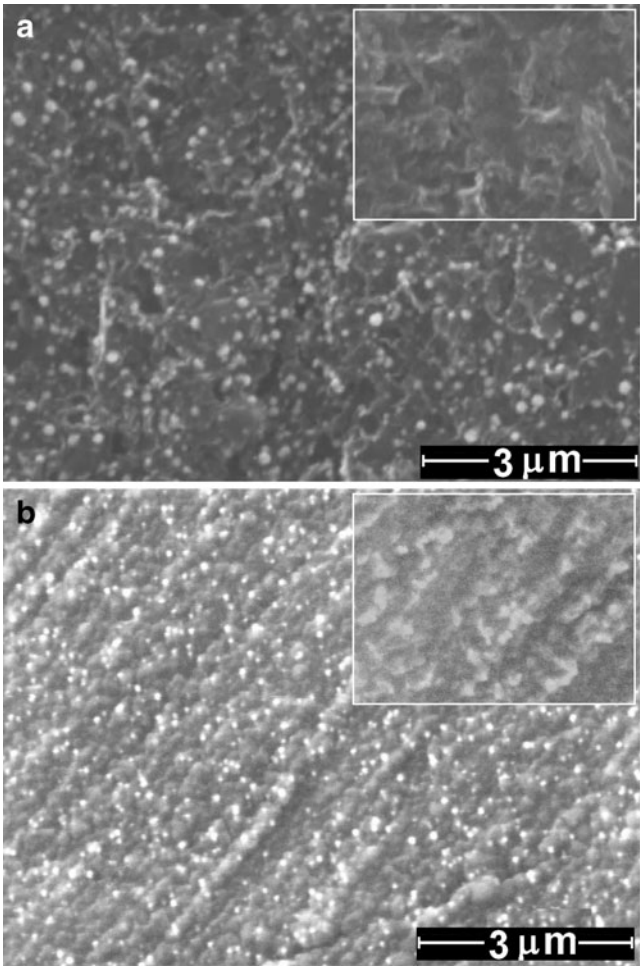

Fig. 2 SEM images of **a** Pt/G and **b** Pt/PTy/G electrodes, obtained after the stabilization of the voltammetric response. Platinum loadings ($mg\,cm^{-2}$): **a** 0.15; **b** 0.12. *Insets*: micrographs of the corresponding substrates before Pt deposition

three pairs of doublets (Fig. 3a). The most intense doublet (at 71.5 and 74.9 eV) is the signature of metallic Pt. The second doublet (at 72.8 and 76.8 eV) could be assigned to Pt(II) oxidation state which is most likely present as Pt $(OH)_2$ [54, 55]. The third doublet, at even higher BE (at 74.1 and 77.2 eV), can be ascribed to the presence of a mixture of Pt(II) and Pt(IV) oxides [54, 55]. Indeed, we have to emphasize that under our experimental conditions it was not possible to discriminate between PtO and PtO_2. A comparison of oxidation state relative concentrations of Pt (0), $Pt(OH)_2$, and Pt oxides put into evidence the fact that on the surface of the Pt/G electrodes, platinum was predominantly (74.1%) in its elemental form.

Figure 3b shows the 4f spectrum obtained for the Pt deposited on the PTy-modified graphite substrate. Here again, the Pt 4f spectrum could be fitted by the same three pairs of overlapping Gaussian–Lorentzian curves, and it appears that, unlike Pt/G case, on the surface of the Pt/PTy/G electrodes $Pt(OH)_2$ species prevail among the platinum chemical states (see Table 1). It is also worthy to note that, in the XPS data processing for both Pt/G and Pt/PTy/G, the ratio $4f_{7/2}/4f_{5/2}$ areas and the spin–orbit splitting values were constrained to 4/3 and 3.35 eV, respectively, according to the theory findings [56].

In order to check the activity for the oxidation of the methanol of the Pt–PTy composite, cyclic voltammetric measurements (scan rate, 50 $mV\,s^{-1}$) were performed within the potential range 0.0–1.2 V in a 0.5 M H_2SO_4 deaerated solution in the presence of 2.25 M CH_3OH. Reproducible voltammetric signals were obtained after approximately five consecutive cycles, and Fig. 4 shows characteristic voltammetric patterns recorded both for a Pt/G electrode (curve 1) and for a Pt/PTy/G one (curve 2).

It is worthy to note that the platinum loadings of the two electrodes were slightly different (0.17 $mg\,cm^{-2}$ for Pt/G and 0.13 $mg\,cm^{-2}$ for Pt/PTy/G) and the voltammograms for Fig. 4 were normalized by taking into account the estimated average values of the specific surface area (i.e.,

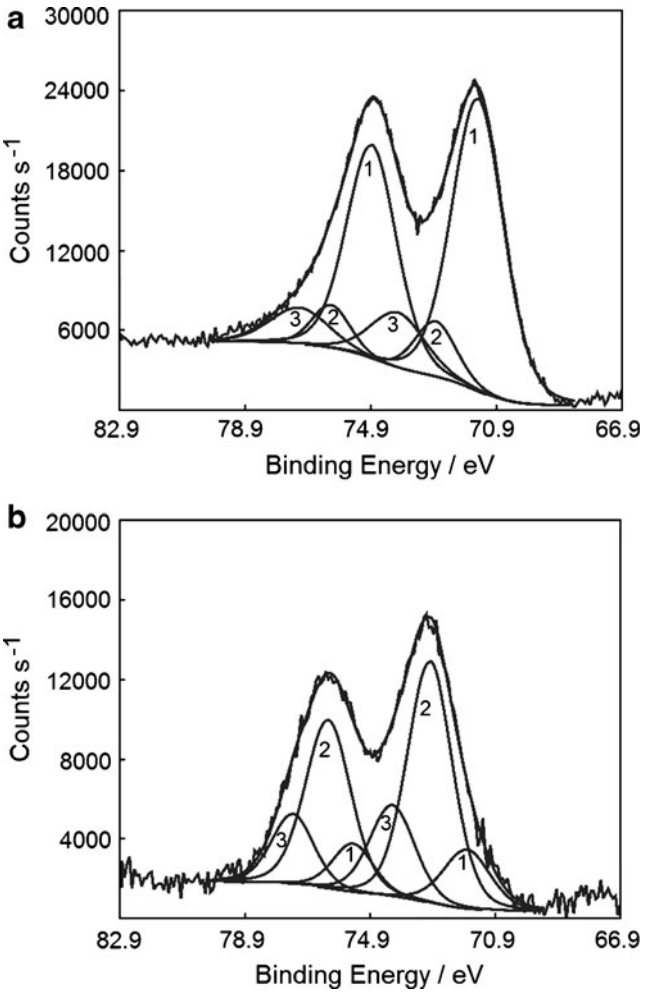

Fig. 3 Deconvoluted Pt 4f XPS spectra of **a** Pt/G and **b** Pt/PTy/G, fitted by the three pairs of overlapping Gaussian–Lorentzian curves that are assigned to *1* Pt(0), *2* $Pt(OH)_2$, and *3* Pt oxides

Table 1 Binding energies and relative intensities of different platinum species on the surface of Pt/G and Pt/PTy/G

Sample	Species	Binding energy (4f7/2; eV)	Oxidation states relative concentration (%)
Pt/G	Pt(0)	71.5	74.1
	$Pt(OH)_2$	72.8	11.2
	Pt oxides	74.1	14.6
Pt/PTy/G	Pt(0)	71.6	15.5
	$Pt(OH)_2$	72.8	61.2
	Pt oxides	74.0	23.2

4.5 and 54 $m^2 g^{-1}$ for Pt/G and Pt/PTy/G, respectively). The peak current density corresponding to methanol oxidation during the anodic scan is approximately 2.5 times lower at the Pt/PTy/G electrodes (curve 2) than at the Pt/G ones (curve 1). This behavior suggests that the presence of PTy results in a decrease of the activity of the catalyst, probably due to the fact that, as SEM measurements indicated, some of the platinum particles are deposited into rather narrow pores of the polymer and are less accessible to methanol. Figure 4 also shows that at the Pt/PTy/G electrodes the voltammetric peak recorded during the anodic scan is shifted towards higher potential values. It is reasonable to ascribe this behavior to the presence of the PTy coating which leads not only to a partial deactivation of the electrocatalyst, but also to a non-negligible ohmic resistance. We have found, however, that these drawbacks are largely compensated by the fact that the specific surface area of the Pt particles is approximately ten times higher when deposited on PTy-covered graphite. This feature is clearly illustrated by the inset from Fig 4, where the current was expressed in terms of mass activity (MA) (measured current divided by the deposited Pt mass). It appears that the use of PTy as substrate for platinum allows obtaining an efficiency of the electrocatalyst utilization approximately three times higher than that available with Pt/G electrodes (compare curves 2 and 1 from the inset in Fig. 4). The mean value of the mass activity obtained with the Pt/PTy/G electrodes (ca. 85 $A g^{-1}$) is encouraging because it compares favorably with those available when using other graphite supported Pt-polymer composites, involving polyaniline [57, 58], polypyrrole [16], or polyindole [59]. Nevertheless, this value is still below those obtainable with substrates such as polyaniline nanowires [60], polypyrrole-modified carbon nanotubes [16], or polyaniline layers containing carbon black particles [58]. This behavior suggests that the mass activity of the Pt–PTy composite could be improved to some extent by depositing the polymer matrix on some high surface area support, such as carbon powder. However, this aspect will be addressed in future work.

To better understand the influence of the polymer substrate on the electrocatalytic properties of the Pt particles, EIS measurements were also carried out in a 0.5 M H_2SO_4+3.7 M CH_3OH solution, both at Pt/G and Pt/PTy/G electrodes, and typical results (normalized by the corresponding active surface area) are illustrated in Fig. 5

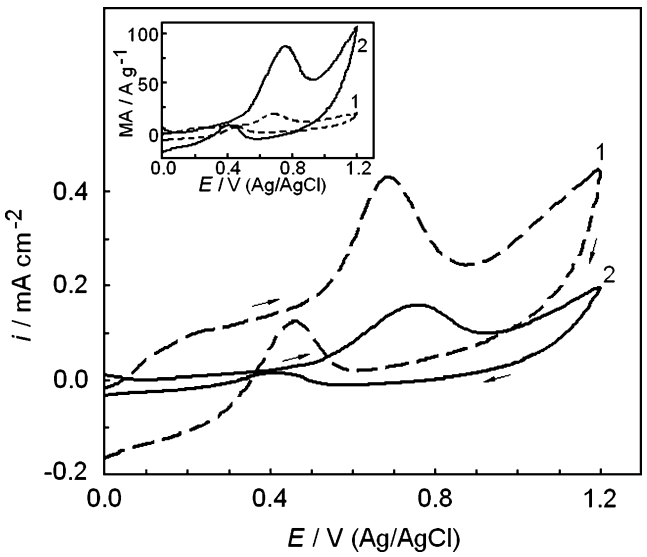

Fig. 4 Stable voltammetric responses in 0.5 M H_2SO_4+2.25 M CH_3OH deaerated solution for *1* Pt/G and *2* Pt/PTy/G electrodes recorded at a scan rate of 50 $mV s^{-1}$ and normalized by the estimated active surface area. Platinum loadings ($mg cm^{-2}$): *1*—0.17, *2*—0.13. *Inset*: cyclic voltammograms expressed in terms of mass activity (MA)

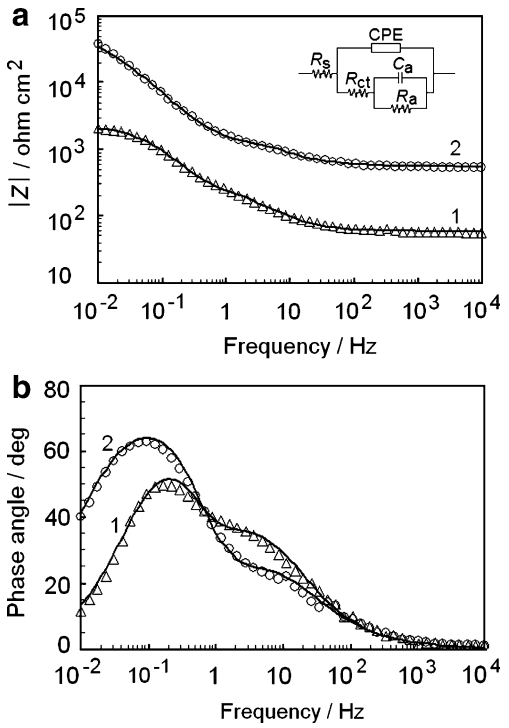

Fig. 5 Representative Bode plots obtained in 0.5 M H_2SO_4+3.7 M CH_3OH at an applied potential of 0.6 V for *1* Pt/G and *2* Pt/PTy/G electrodes: **a** variation of the impedance magnitude; **b** variation of the phase angle. Platinum loadings ($mg cm^{-2}$): *1*—0.13, *2*—0.12. *Solid lines* show the results of the simulation. *Inset*: equivalent circuit

by curves 1 and 2, respectively. For both electrodes, the Bode plots exhibit a hump within the frequency range from 2 to 40 Hz. This behavior (better evidenced by the variation of the phase angle from Fig. 5b) suggests that the response in the investigated frequency range can be simulated by an equivalent circuit predicting two time constants, similar to those generally used for electrode processes that involve intermediates adsorption/desorption equilibria [61–63]. This equivalent circuit is shown in the inset from Fig. 5a and includes the resistance of the solution (Rs), the charge transfer resistance (Rct), the adsorption pseudocapacitance (Ca), and the resistance imposed by the reaction intermediates adsorbed at the electrode (Ra).

Due to the roughness of the electrode surface and to its possible physical nonuniformity, a constant phase element was used to simulate the capacitance of the double layer.

Elucidating the mechanism of methanol oxidation at the Pt–PTy composite is a difficult task and was beyond the scope of the present work. It is worthy to note, however, that within the investigated potential range (0.5–0.7 V) a good agreement was found between experimental and calculated EIS data (chi-square lower than 10^{-3}), which allowed us to reliably estimate the parameters of the equivalent circuit. We should emphasize that the EIS results obtained in this work cannot be used directly to infer mechanistic details, due to the lack of additional experimental data and to some uncertainty related to exact determination of the real active surface area of the catalytic deposits. Nevertheless, it was found that, even compared on a relative basis, these results could explain to some extent the effect of the PTy matrix on the electrochemical behavior of the deposited Pt particles.

Figure 6 shows the variation of Rct and Ca as a function of the applied potential, both for Pt/G (Fig. 6a) and for Pt/PTy/G (Fig. 6b) electrodes. As expected, over the whole investigated potential range, the charge transfer resistance corresponding to CH_3OH oxidation is higher at Pt/PTy/G, in line with the partial deactivation of the Pt particles from the polymer matrix evidenced by the cyclic voltammetric experiments (see above). It can be seen that, for both types of electrodes, the increase of the anodic potential up to ca. 0.6 V leads to an enhancement of the reaction rate (lower Rct), while higher values of the applied potential result in an increase of the charge transfer resistance (curves 1 from Fig. 6a, b), most likely due to the blockage of the reaction sites by adsorbed intermediates (see [64] and references therein). It appears however that this increase is more significant at the Pt/G electrodes, suggesting that the platinum electrocatalyst on PTy substrate is less sensitive to deactivation compared to platinum on graphite.

It is also interesting to observe that at the Pt/G electrodes the adsorption Ca increases with increasing potential (curve 2 from Fig. 6a) indicating an increase of the surface

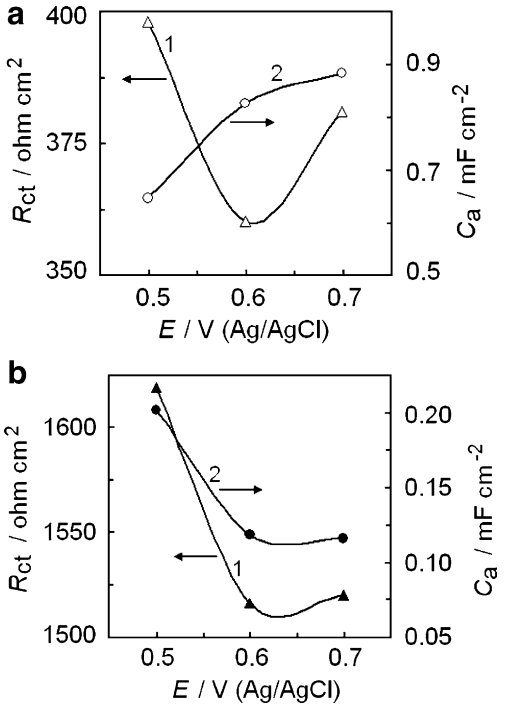

Fig. 6 *1* Variation of charge transfer resistance and *2* adsorption pseudocapacitance as a function of the applied potential, as calculated from the EIS results for **a** Pt/G and **b** Pt/PTy/G electrodes

coverage by the reaction intermediates. The fact that the estimated values of Ca are higher for the Pt/G electrodes is further proof of stronger adsorption processes at platinum particles deposited on bare graphite. A different behavior was found for the Pt/PTy/G electrodes, in which case the decrease of Ca (curve 2 from Fig. 6b) also supports the conclusion that the overall methanol oxidation process is less affected by the adsorption of intermediates, when the Pt particles are immobilized into the PTy matrix. It is reasonable to ascribe this behavior to the much higher concentration of $Pt(OH)_2$ at the Pt–PTy composite surface, evidenced by the XPS measurements (see above). These Pt–OH species could be available to assist in the oxidation of strongly bond CO on the platinum particle surfaces [65], resulting in an increased resistance to fouling.

The activity of the Pt–PTy composite for methanol oxidation was also checked by polarization measurements, performed in a 0.5 M H_2SO_4+3.7 M CH_3OH solution at an applied potential of 0.6 V. It is likely that under these experimental conditions, the overall anodic current could include a non-negligible charging contribution. This is why the methanol oxidation current was calculated as the difference between the current recorded in the presence and in the absence of CH_3OH. The variation of the oxidation current as a function of time is illustrated in Fig. 7 by the chronoamperometric curve for a Pt/PTy/G electrode with a platinum loading of 0.12 mgcm^{-2} (curve

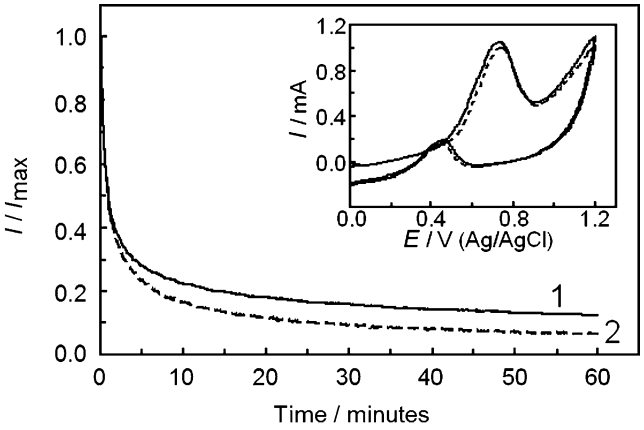

Fig. 7 Variation of the methanol oxidation current as a function of time for *1* Pt/PTy/G and *2* Pt/G electrodes. Solution, 0.5 M H_2SO_4+ 3.7 M CH_3OH; applied potential, 0.6 V. Platinum loadings (mg cm^{-2}): *1*—0.12, *2*—0.15. *Inset*: cyclic voltammograms (recorded under the same experimental conditions as in Fig. 4) at a Pt/PTy/G electrode (Pt loading, 0.09 mg cm^{-2}) before (*solid line*) and after (*dotted line*) 2 h of continuous methanol oxidation (see text)

1). Figure 7 also shows, for comparison, a typical response under the same experimental conditions for a Pt/G electrode (Pt loading, 0.15 mg cm^{-2}) obtained by platinum electrodeposition on bare graphite (curve 2). It should be noted that, although the Pt loadings are comparable, Pt/PTy/G and Pt/G electrodes are inherently different in terms of surface area which results in different values of the instantaneous current. This is why, in order to put into better perspective the results of the polarization measurements, in Fig. 7 the methanol oxidation current (I) was normalized by its maximum value (I_{max}).

In the early stage of the electrolysis, a rather sharp decrease of the oxidation current was observed for the two types of electrodes. However, during further polarization this decrease tends to become slower for the Pt/PTy/G electrodes and, after ca. 15 min, the oxidation current reaches ~20% of its initial value while that for the Pt/G electrodes decreases to ~12%. This is an indication of the fact that during CH_3OH oxidation in acidic media Pt–PTy composite is slightly less sensitive to deactivation, e.g., via CO poisoning, compared to platinum on graphite. These findings are in line with the results of the EIS measurements and allow us to conclude that, from the standpoint of the resistance to fouling, there is a slight, but nonetheless significant, inherent advantage of the PTy substrate.

In order to assess the practical utility of the Pt–PTy composite as electrode material for methanol oxidation more detailed long-term polarization measurements are in progress. We should note, however, that our preliminary results concerning the stability of the Pt/PTy/G electrodes are rather promising, as suggested by the inset in Fig. 7. Thus, it was observed that for a Pt/PTy/G electrode (Pt loading, 0.09 mg cm^{-2}), after 2 h of continuous polarization at 0.6 V in a 0.5 M H_2SO_4+3.7 M CH_3OH solution, the peak current corresponding to methanol oxidation during the anodic scan decreased with less than 6%. However, an anodic shift (ca. 8 mV) of the same peak was also put into evidence (see the dotted curve from the inset in Fig. 7) indicating a slight deactivation of the electrocatalyst.

It is difficult to explain this result without further detailed work. However, it is likely that the high concentration of Pt$(OH)_2$ at the composite surface plays a critical role in ensuring better stability during methanol oxidation of the Pt/PTy/G electrodes. Although the reason for which Pt–OH species are preferentially formed on the PTy substrate is an issue that remains to be addressed, we can offer some speculative explanation that could provide a basis for additional experiments. Thus, it seems reasonable to assume that, as the schematic diagram from Fig. 8 tentatively illustrates, this behavior could be the result of the presence of free amine groups in the PTy matrix, in proximity to Pt nanoparticles.

Briefly, potentiodynamic oxidation of tyramine leads to the formation of a polymer with strong polycationic nature, due to the protonation of amino groups [66]. A large amount of anions from the supporting electrolyte is electrostatically associated to NH_4^+ moieties, and each ion

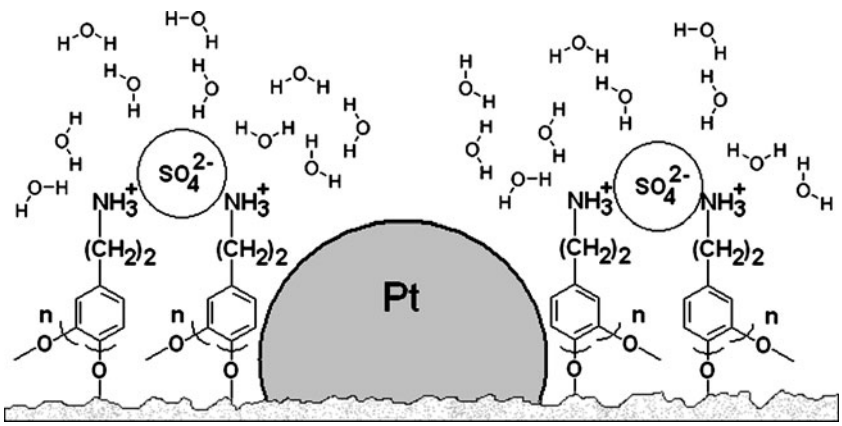

Fig. 8 Schematic diagram tentatively explaining the role of the amine groups from the PTy in promoting the formation of Pt–OH species

pair is very likely solvated by water molecules [67]. This bound water could enhance the formation of Pt–OH species which can further react with adsorbed CO [65].

A second possibility that cannot be ruled out when attempting to explain the slower deactivation of the Pt/PTy/G electrodes is simply that the PTy surface has a much lower tendency to adsorb reaction products and intermediates, which could otherwise create a "reverse spillover" effect, fouling the platinum surface.

Conclusions

Anodic oxidation of tyramine in acidic media, followed by the electrochemical deposition of platinum, allowed us to establish a straightforward method to obtain a composite that exhibits both high specific surface area of the Pt nanoparticles and promising electrocatalytic properties for methanol oxidation, even with Pt loadings as low as 0.12 $mg\,cm^{-2}$. The method is also noteworthy because it allows the preparation of large-area electrodes at ambient temperature, with essentially no need for time-consuming pretreatment procedures. Cyclic voltammetric experiments have shown that the presence of the PTy intermediary layer leads to a partial deactivation of the Pt particles. Nevertheless, this drawback is largely compensated by the significant enhancement of the active surface area. This is why, the use of PTy-modified graphite as substrate for platinum electrodeposition allows achieving much higher efficiency of the electrocatalyst utilization. The results of the EIS and chronoamperometric measurements suggest that, when deposited on a polytyramine substrate, platinum may be slightly less susceptible to deactivation, e.g., via CO poisoning, during CH_3OH oxidation. This behavior was tentatively ascribed to the presence of a large amount of Pt–OH species at the Pt–PTy composite surface (as evidenced by the XPS measurements), or to a less significant adsorption of reaction intermediates that could foul the Pt surface. These are issues that remain to be addressed and are currently being pursued in our laboratory. However, these findings are of particular interest because they indicate that by using PTy as a support it is possible, at least in principle, to minimize the loading of alloying metals such as, e.g., ruthenium, while maintaining high catalytic activity. Finally, we should note that many representative conducting polymers, including polyaniline and polypyrrole, are not as yet free of problems, related to chemical degradation during metal particles deposition or during methanol oxidation (see [68] and references therein). This is further reason for the investigation of new metal–polymer systems, among which the Pt–PTy composite appears to be highly worthy of development.

References

1. Antolini E (2003) J Mater Sci 38:2995
2. Kangasniemi KH, Condit DA, Jarvi TD (2004) J Electrochem Soc 151:E125
3. Ralph TR, Hogarth MP (2002) Platinum Met Rev 46:117
4. Carmo M, Paganin VA, Rosolen JM, Gonzalez ER (2005) J Power Sources 142:169
5. Kongkanand A, Kuwabata S, Girishkumar G, Kamat P (2006) Langmuir 22:2392
6. Prabhuram J, Zhao TS, Tang ZK, Chen R, Liang ZX (2006) J Phys Chem B 110:5245
7. Wang X, Li W, Chen Z, Waje M, Yan Y (2006) J Power Sources 158:154
8. Han DM, Guo ZP, Zeng R, Kim CJ, Meng YZ, Liu HK (2009) Int J Hydrogen Energy 34:2426
9. Maiyalagan T (2009) Int J Hydrogen Energy 34:2874
10. Bennett JA, Show Y, Wang S, Swain GM (2005) J Electrochem Soc 152:E184
11. Suffredini HB, Tricoli V, Vatistas N, Avaca LA (2006) J Power Sources 158:124
12. Siné G, Smida D, Limat M, Foti G, Comninellis C (2007) J Electrochem Soc 154:B170
13. Salazar-Banda GR, Eguiluz KIB, Avaca LA (2007) Electrochem Commun 9:59
14. Spătaru N, Zhang X, Spătaru T, Tryk DA, Fujishima A (2008) J Electrochem Soc 155:B264
15. Choi JH, Park KW, Lee HK, Kim YM, Lee JS, Sung YE (2003) Electrochim Acta 48:2781
16. Selvaraj V, Alagar M (2007) Electrochem Commun 9:1145
17. Chang TK, Wen TC (2008) Synth Met 158:364
18. Huang LM, Wen TC (2008) J Power Sources 182:32
19. Habibi B, Pournaghi-Azar MH, Abdolmohammad-Zadeh H, Razmi H (2009) Int J Hydrogen Energy 34:2880
20. Santhosh P, Gopalan A, Lee KP (2006) J Catal 238:177
21. Liu FJ, Huang LM, Wen TC, Gopalan A (2007) Synth Met 157:651
22. Kim S, Park SJ (2008) Solid State Ionics 178:1915–1921
23. Bavio MA, Kessler T, Castro-Luna AM (2008) J Colloid Interface Sci 325:414
24. Liu FJ, Huang LM, Wen TC, Li CF, Huang SL, Gopalan A (2008) Synth Met 158:767
25. Palmero S, Colina A, Muñoz E, Heras A, Ruiz V, Lopez-Palacios J (2009) Electrochem Commun 11:122
26. Selvaraj V, Alagar M, Hamerton I (2006) J Power Sources 160:940
27. Zhao H, Li L, Yang J, Zhang Y, Li H (2008) Electrochem Commun 10:876
28. Zhao H, Li L, Yang J, Zhang Y (2008) J Power Sources 184:375
29. Maiyalagan T (2008) J Power Sources 179:443
30. Jiang C, Lin X (2007) J Power Sources 164:49
31. Kuo CW, Huang LM, Wen TC, Gopalan A (2006) J Power Sources 160:65
32. Hu ZA, Ren LJ, Feng XJ, Wang YP, Yang YY, Shi J, Mo LP, Lei ZQ (2007) Electrochem Commun 9:97
33. Huang LM, Tang WR, Wen TC (2007) J Power Sources 164:519
34. Liu FJ, Huang LM, Wen TC, Gopalan A, Huang JS (2007) Mater Lett 61:4400
35. Liu FJ, Huang LM, Wen TC, Li CF, Huang SL, Gopalan A (2008) Synth Met 158:603
36. Kuo CW, Sivakumar C, Wen TC (2008) J Power Sources 185:807
37. Lofrano RC, Madurro JM, Romero JR (2000) J Mol Catal A Chem 153:237
38. Lofrano RCZ, Madurro JM, Abrantes LM, Romero JR (2004) J Mol Catal A Chem 218:73
39. Losic D, Cole M, Thissen H, Voelcker NH (2005) Surf Sci 584:245

40. Situmorang M, Gooding JJ, Hibbert DB, Barnett D (2001) Electroanalysis 13:1469
41. Tenreiro A, Cordas CM, Abrantes LM (2003) Port Electrochim Acta 21:361
42. Wu ZS, Li JS, Deng T, Luo MH, Shen GL, Yu RQ (2005) Anal Biochem 337:308
43. Miscoria SA, Barrera GD, Rivas GA (2006) Sens Actuators B 115:205
44. Castro CM, Vieira SN, Goncalves RA, Brito-Madurro AG, Madurro JM (2008) J Mater Sci 43:475
45. Spătaru T, Marcu M, Banu A, Roman E, Spătaru N (2008) Rev Chim 59:1366
46. Spătaru T, Marcu M, Banu A, Roman E, Spătaru N (2009) Electrochim Acta 54:3316
47. Long JW, Swider KE, Merzbacher CI, Rolison DR (1999) Langmuir 15:780
48. Ross PN Jr (1979) J Electrochem Soc 126:67
49. Shimazu K, Weisshaar D, Kunawa T (1987) J Electroanal Chem 223:223
50. Xiong L, Manthiram A (2004) Electrochim Acta 49:4163
51. Mentus SV (2005) Electrochim Acta 50:3609
52. Park KW, Choi JH, Ahn KS, Sung YE (2004) J Phys Chem B 108:5989
53. Chan BC, Liu R, Jambunathan K, Zhang H, Chen G, Mallouk TE, Smotkin ES (2005) J Electrochem Soc 152:A594
54. Moulder JF, Stickle WF, Sobol PE, Bomben KD (1995) Handbook of X-Ray Photoelectron Spectroscopy, Physical Electronics, Eden Prairie, MN
55. NIST X-Ray Photoelectron Spectroscopy Database, Version 4.0, National Institute of Standards and Technology, Gaithersburg, 2008.
56. Fairley N (2003) In: Briggs D, Grant J (eds) Surface analysis by Auger and X-ray photoelectron spectroscopy. IM Publications, Manchester
57. Yano J, Shiraga T, Kitani A (2008) J New Mater Electrochem Syst 11:235
58. Wu G, Li L, Li JH, Xu BQ (2005) Carbon 43:2579
59. Nagashree KL, Raviraj NH, Ahmed MF (2010) Electrochim Acta 55:2629
60. Liu FJ, Huang LM, Wen TC, Li CF, Huang SL, Gopalan A (2008) Synth Met 158:767
61. Ho JCK, Tremiliosi Filho G, Simpraga R, Conway BE (1994) J Electroanal Chem 366:147
62. Franco DV, DaSilva LM, Jardim WF, Boodts JFC (2006) J Braz Chem Soc 17:746
63. Orazem ME, Tribollet B (2008) Electrochemical Impedance Spectroscopy. Wiley, Hoboken
64. Campos CL, Roldan C, Aponte M, Ishikawa Y, Cabrera CR (2005) J Electroanal Chem 581:206
65. Léger JM (2001) J Appl Electrochem 31:767
66. Tran LD, Piro B, Pham MC, Ledoan T, Angiari C, Dao LH, Teston F (2003) Synth Met 139:251
67. Tenreiro AM, Nabais C, Correia JP, Fernandes FMSS, Romero JR, Abrantes LM (2007) J Solid State Electrochem 11:1059
68. Antolini E, Gonzalez ER (2009) Appl Catal A—Gen 365:1